

Solvation dynamics in viscous polymer solution: Propylene carbonate confined by poly(methylmethacrylate)

Fang He and Ranko Richert

Department of Chemistry and Biochemistry, Arizona State University, Tempe, Arizona 85287-1604, USA

(Received 17 April 2006; revised manuscript received 25 May 2006; published 6 July 2006)

Solvation dynamics of a triplet state probe is used to explore the dynamics of supercooled propylene carbonate (PC) when modified by the presence of poly(methyl methacrylate) (PMMA) in viscous polymer solution. In the PMMA weight fraction range 0 to 0.32, the relaxation time for dipolar solvation increases by a factor of approximately 1500, if evaluated at a constant temperature. This is equivalent to a shift of the PC glass-transition temperature T_g by +6.4 K as a result of geometrical restriction by the presence of 32 wt. % PMMA. In terms of the estimated average PC-PMMA distance, the relaxation time approaches the bulk value much more rapidly compared with size effects of confinement in porous glasses or microemulsion droplets. The interpretation of this feature is that a reduced PMMA concentration not only increases the average PC-PMMA distance, but also changes from a solid to a more open topology of the confining material. Accordingly, the slowest dynamics in these mixtures are not found near a single polymer chain, but only in the more concentrated polymer environments where a larger fraction of the cooperative volume is immobilized by macromolecules.

DOI: [10.1103/PhysRevB.74.014201](https://doi.org/10.1103/PhysRevB.74.014201)

PACS number(s): 64.70.Pf, 68.08.-p, 77.22.Gm

I. INTRODUCTION

Supercooled liquids combine the irregular structure of normal liquids with viscosities which can be more reminiscent of the solid state.¹ In the viscous regime near the glass transition temperature T_g , it requires a considerable distance between two molecules for them to relax independently. Such a length scale inherent in the supercooled state of liquids is often associated with the size ξ of cooperatively rearranging regions (CRR's),² or with the domain sizes related to dynamic heterogeneity.³⁻⁵ In either case, length scales around a few nanometers are typically reported.^{6,7} As a result, it is not surprising that such liquids are particularly sensitive to geometrical confinement if the spatial restriction approaches the several nanometer range. Confinement effects on molecular liquids near their glass transition have been investigated extensively,⁸⁻¹² but no unifying picture has emerged from the observations yet.^{13,14} As in the original observation, confinement effects are often reported as a change in the glass transition temperature T_g .¹⁵ For practical purposes, T_g is usually defined by a threshold value of the viscosity ($\eta=10^{12}$ Poise) or of the relaxation time ($\tau_0=10^2$ s).¹⁶ Therefore, a certain confinement induced ΔT_g translates into a concomitant change of the time scale of structural relaxation or viscous flow, provided that amplitude and correlation pattern are approximately preserved.¹⁷ Such changes in the time scale of molecular motion will alter the transport properties of liquids near surfaces, interfaces, or membranes and in restricting geometries such as rocks, clay, or other porous materials.

Among many others techniques, solvation dynamics experiments have been employed in order to gain further insight into the effects geometrical confinement has on the dynamics of liquids.¹⁸⁻²⁰ The triplet state variant of this optical technique is specifically designed to address the slow relaxation features of viscous liquids near their glass transition.^{21,22} In recent studies, we have used triplet state

solvation techniques for studying the dynamics of confined liquids at the liquid/solid interface,²³ and for comparing hard versus soft boundary conditions.^{24,25} These observations could all be rationalized on the basis of modified dynamics at the interface, with the effect penetrating into the liquid on a length scale which agrees with that of cooperativity. The interfacial relaxation times were around three decades away from the bulk counterpart, slower in the case of "hard" confinement and faster in the case of "soft" confinement. Effect other than those related to the surface, i.e., true "finite size" effects, did not need to be considered. Dramatic changes of the relaxation time at interfaces are restricted to the cases of supercooled liquids,²⁶ while more fluid system display smaller relaxation time changes,²⁷ which do not extend away from the surface.²⁸ This can be attributed to a reduced length scale of cooperative effects at the higher temperatures, where ξ is not expected to exceed the dimensions of a molecule significantly.²⁹

Near a solid interface, e.g., in a porous glass, a significant fraction of the cooperative volume of the liquid is replaced by immobile material, leading to the strongly altered dynamics mentioned above. On the other hand, a single guest molecule has little or no effect on the surrounding dynamics, even if its mobility is greatly reduced relative to the liquid. Polymer solutions at different concentrations provide intermediate situations, allowing one to assess the impact of the size of a rigid obstacle (in terms of the fraction of cooperative volume) required for the dynamics to change by orders of magnitude.

In the present work, we ask whether the case of moderately hard confinement in terms of polymer solutions can also be rationalized on the basis of certain interfacial conditions which extend few nanometers into the liquid. As a result of a dielectric study of the dynamics of a molecular liquid as part of a polymer solution, Svanberg *et al.* have suggested that the solvent relaxation time changes systematically as a function of the distance from the polymer chain.³⁰

In order to provide a straightforward comparison with our previous results, triplet state solvation techniques are applied again to explore the confinement effects in a polymer solution, propylene carbonate in poly(methyl methacrylate). It is assumed that the macromolecules act as semirigid barriers to the mobility of the molecular solvent, which is probed by the solvation dynamics experienced by a suitable chromophore. However, randomly scattered polymer chains will not modify the relaxation behavior in the same way as the solid surface of a porous glass. Experimental control over the average length scale of confinement is by the polymer concentration. However, the effect of reducing the polymer content is twofold: it allows for larger solvent pools or larger average distances of the solvent to the nearest polymer chain, and it changes the topology of the confining material from a more connected enclosure to a more open structure. Therefore, the effect of polymer concentration will not necessarily map onto a pore size diameter like dependence of a true three-dimensional geometrical restriction.

II. EXPERIMENTS

The technique of triplet state solvation dynamics requires a dipolar probe dissolved at a low concentration in the system under study.^{22,31} For the present case of a solvent with substantial polarity, quinoxaline (QX, Aldrich, 98%, further purified by sublimation) is employed as a suitable chromophore at a concentration around 2×10^{-4} mol/mol with respect to the molecular solvent. Poly(methyl methacrylate) (PMMA, Aldrich, <5% toluene) with both higher and lower molecular weight ($M_w=996$ kg/mol and 120 kg/mol) has been used as polymer component. The polymer was heated to 450 K under vacuum to eliminate moisture and other volatile impurities before any measurement. Propylene carbonate (PC, Aldrich, 99.7%, anhydrous) was used as received. The glass transition temperature of PC near $T_g=160$ K is much lower than that of PMMA near 380 K. The mixtures of PC (with QX added) with PMMA were prepared and allowed to equilibrate at room temperature for extended periods of time. Heating up to 330 K was required for the higher PMMA concentrations to increase the mobility and accelerate the process of dissolving in PC. At elevated PMMA concentrations the viscosity of the mixture becomes extremely high, which limits this investigation to samples from pure PC to about $w_{\text{PMMA}}=32\%$ PMMA content. The sample is filled into a copper cell with fused-silica window for the optical experiments. This cell is mounted to the cold stage of a closed cycle He refrigerator (Leybold, RDK 10-320, RW 3) and the temperature is measured and stabilized by a controller (Lake Shore, LS 330) equipped with calibrated diode sensors (Lake Shore, DT-470-CU-13).

The key observable in a triplet state solvation study is the time resolved phosphorescence emission spectrum of the probe QX, because the time dependent redshift of the optical emission provides direct information on the solvent dynamics.³² Details of the technique and interpretation have been supplied elsewhere.^{17,19,21,22} In brief, a frequency tripled Nd:YAG laser (Continuum, SLI-10) operated at $\lambda_{\text{exc}}=355$ nm is used to excite the probe molecule at a rep-

etition rate of ≈ 1 Hz. The phosphorescence emission is dispersed by a triple grating polychromator (Acton Research, SpectraPro-275) and registered by a MCP intensified diode array camera (EG&G, 1455B-700-HQ) with controller (EG&G, 1471A), gating options (EG&G, 1304), and synchronization facilities (SRS, DG-535). The system is wavelength calibrated and across the typical redshifts of approximately 300 cm^{-1} the spectral sensitivity is sufficiently flat so that uncorrected emission data is used. The time resolution is defined by gating the camera with gate delays between 10 μs and 1 s, and the gate width being set to $\leq 10\%$ of the delay time. Spectra are recorded by accumulating the signals from typically 300 excitation pulses. The time resolved solvation dynamics experiments all refer to the $T_1 \rightarrow S_0(0-0)$ emission of the probe QX, recorded at logarithmic time increments.

III. RESULTS

In order to determine the relaxation behavior of the solvent, the time resolved $T_1 \rightarrow S_0(0-0)$ emission spectra are analyzed in terms of Gaussian profiles, which provides the average emission energy $\langle \bar{\nu}(t) \rangle$ as a function of time. The limiting values at short and long times determine the total redshift $\Delta \bar{\nu} = \langle \bar{\nu}(t=0) \rangle - \langle \bar{\nu}(t \rightarrow \infty) \rangle$, which is $\Delta \bar{\nu}_{\text{bulk}} = 355 \text{ cm}^{-1}$ for bulk PC. This comparatively large value for the probe QX originates from the large dipole moment (≈ 5 D) and dielectric constant (≈ 83) of PC in its viscous regime. Scaling the average emission energies to their limiting values yields the solvation (or Stokes-shift) correlation function

$$C(t) = \frac{\langle \bar{\nu}(t) \rangle - \langle \bar{\nu}(\infty) \rangle}{\langle \bar{\nu}(0) \rangle - \langle \bar{\nu}(\infty) \rangle}, \quad (1)$$

which reflects the (normalized) structural relaxation behavior of the liquid.

An example for the time and temperature dependence of $C(t)$ is shown in Fig. 1 for the QX/PC/PMMA sample at a concentration of $w_{\text{PMMA}}=6.25\%$. The solvent response is best characterized by fitting the resulting $C(t)$ curves with suitable relaxation functions. In the case of viscous liquids, $C(t)$ decays deviate strongly from purely exponential patterns and often follow a stretched exponential or Kohlrausch-Williams-Watts (KWW) functions

$$C(t) = \exp \left[- \left(\frac{t}{\tau_0} \right)^\beta \right]. \quad (2)$$

Such a fit quantifies the characteristic relaxation time scale by τ_0 and the degree of nonexponentiality by the exponent β with $0 < \beta \leq 1$. Within the limited experimental temperature ranges, the stretching exponent β is not expected to change significantly with temperature, and the KWW fits in Fig. 1 thus use a common exponent $\beta=0.4$. The main effect of temperature is to alter the relaxation time constant τ_0 , which amounts to a factor of >5 per Kelvin in the present example.

Typically, the time scale of structural relaxation in supercooled liquids changes in a super-Arrhenius fashion. In many cases, the value of τ_0 depends on temperature according to the Vogel-Fulcher-Tammann (VFT) law

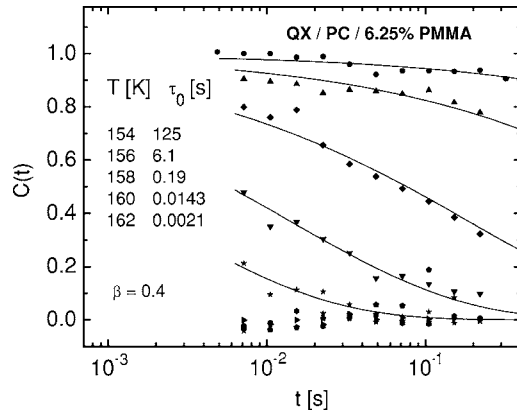


FIG. 1. Time resolved solvation correlation function $C(t)$ for QX in a 6.25% PMMA in PC mixture. The symbols are experimental results for different temperatures as listed from top to bottom curve. These data are used to determine the values for τ_0 and β according to Eq. (2). The resulting KWW fits are represented by solid lines and calculated using a common value of $\beta=0.4$ and the relaxation times τ_0 compiled in the legend.

$$\log_{10}(\tau_0/\text{s}) = A + B/(T - T_0). \quad (3)$$

In the case of our PC/PMMA mixtures, VFT like behavior is observed in Fig. 2, consistent with the position and curvature of dielectric relaxation data for bulk PC.³³ The dashed line in this graph represents a VFT fit to the bulk PC solvation data, using the parameters $A=-16.0$, $B=405$ K, and $T_0=133.4$ K. As obvious from Fig. 2, the dominant effect of composition is to shift the curves towards longer relaxation times as the PMMA content is increased. Within the limitations of the solvation experiment, this frustration effect is not strongly dependent on temperature. In order to quantify this composition dependent feature with a single variable, a temperature $T'=162$ K is selected for which relaxation times are avail-

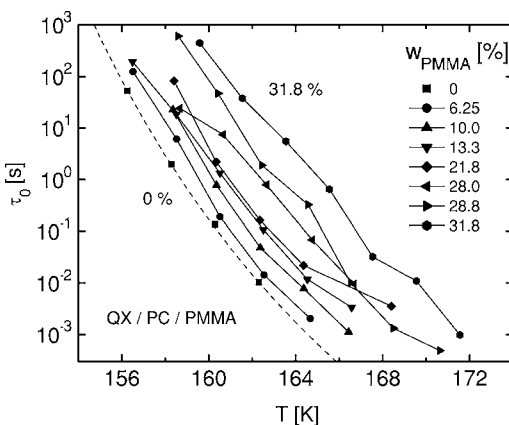


FIG. 2. Temperature dependent solvation times $\tau_0(T)$ of QX in PC/PMMA mixtures of various compositions between 0 and 31.8 % PMMA weight fraction as indicated in the legend. Errors of $\log_{10}(\tau)$ range from 0.1 around $\tau=0.1$ s to 0.6 at much faster and slower times, with the latter cases relying more on fixing the remaining parameters. Symbols represent the experimental results, solid lines serve as guide only, the dashed line is a VFT fit to the bulk PC data with $A=-16.0$, $B=405$ K, and $T_0=133.4$ K.

able across the entire experimental range of compositions. The relaxation times determined at this particular temperature are compiled as τ'_0 in Table I.

Other relevant composition dependent results also compiled in Table I are: the total redshift $\Delta\bar{\nu}$ experienced by QX in the mixture, the glass transition temperature T_g based upon the $\tau=100$ s criterion, the above relaxation time τ'_0 , the KWW or stretching exponent β derived from analyzing the $C(t)$ functions, and the logarithmic relaxation time τ_0 relative to the bulk value, $\log_{10}(\tau_0/\tau_{\text{bulk}})$. The composition effect on the relaxation time τ'_0 is shown in Fig. 3, while the dependence of the total redshift $\Delta\bar{\nu}$ and of the KWW exponent β on concentration are plotted in Fig. 4.

It should be noted that two different molecular weights have been used in this investigation. At low PMMA concentration, a high molecular weight was required to prevent phase separation which became obvious by the opaque appearance of the sample. At high PMMA content, a low molecular weight accelerated the processes of dissolving and flowing. The dependence of T_g on molecular weight can be accounted for with the equation $T_g = T_g(\infty) - K/M_n$,³⁴ where the constant K is of the order 10^5 K g mol⁻¹ and $T_g(\infty) = 378$ K for PMMA. Accordingly, there is only a small T_g shift of about 0.5–1 K between the $M_w=996$ kg/mol and 120 kg/mol PMMA samples. In order to check whether molecular weight altered the properties of the system, samples with the same concentration for the higher and lower molecular weight were made. They showed identical dynamics within the experimental uncertainty.

IV. DISCUSSION

Experimental approaches to the effects of geometrical restriction and proximity of interfaces on liquid dynamics have used many different techniques,^{10–12,35–41} confining geometries,^{42–44} and surface properties.^{14,19,45} Therefore, it is not surprising that the confinement situation is not entirely characterized by a reduced spatial dimension like pore diameter. In fact, many observations demonstrate the importance of the particular condition at the boundary or interface, where the liquid under study is in contact with the confining material. In the case of porous glasses, surface treatment has been shown to alter the dynamics of the liquid, with only little change in the size.^{20,46} A particularly clear case is our recent comparison of hard and soft boundaries, where the glass transition shift can be several Kelvin positive or negative for the same size of the confinement, but with the interface being a rigid glass or more fluid than the confined liquid.²⁵

Additional relevant features are the dimensionality of the geometrical restriction and the topology of the confining material.⁴⁷ In the present context, topology refers to the structure of the confining geometry, e.g., solid surface, more open network such as a polymer gel, or just the occurrence of small immobile obstacles within the liquid. An uninterrupted rigid surface can increase the relaxation time by several orders of magnitude relative to the bulk liquid.²³ On the other hand, individual molecules which are somewhat larger than the liquid constituents can be practically immobile on the

TABLE I. Characteristic parameters for the solvent dynamics in PC/PMMA mixtures for various compositions. The columns refer to the weight fractions of PMMA (w_{PMMA}) and PC (w_{PC}), the total redshift $\Delta\bar{\nu}$ experienced by QX in the mixture, the glass transition temperature T_g based upon the $\tau=100$ s criterion, the relaxation time τ'_0 at $T'=162$ K, the stretching exponent β , the logarithmic relaxation time relative to the bulk value, and the estimated average PC to nearest PMMA distance x .

w_{PMMA} [%]	w_{PC} [%]	$\Delta\bar{\nu}$ [cm^{-1}]	T_g [K]	τ'_0 [s]	β	$\log_{10}(\tau_0/\tau_{\text{bulk}})$	x [nm]
0.00	100	355	155.0	0.016	0.40	0.00	-
6.25	93.7	319	155.5	0.028	0.40	0.24	0.66
10.0	90.0	297	156.3	0.077	0.36	0.68	0.47
13.3	86.7	275	157.0	0.20	0.34	1.09	0.37
13.8	86.2	227	157.2	0.27	0.34	1.22	0.36
21.8	78.2	240	157.3	0.27	0.34	1.23	0.23
28.0	72.0	215	159.0	1.68	0.35	2.02	0.17
28.8	71.2	176	160.0	6.53	0.25	2.61	0.17
31.8	68.2	227	161.4	24.6	0.31	3.19	0.15

time scale of the liquid's structural relaxation, but their impact on the dynamics of the neighboring liquid molecules is negligible. The latter notion is justified by observing that solvent dynamics are bulklike even in the vicinity of probes which do not reorient on this time scale.^{48,49} Here, the molecular obstacle can be considered rigid, but its overall size or contact area with the liquid is insufficient to alter the dynamics significantly because only a small fraction of the cooperative volume is modified. Polymers or other macromolecular objects are intermediate between the two extremes discussed above, and assessing their impact on confinement is the topic of this discussion.

It is a common observation that solvent molecules have a decreased mobility in the presence of polymeric molecules with higher T_g values.⁵⁰ To examine the polymer concentration effect on the relaxation time, we show the results of τ_0 versus PC weight fraction at $T'=162$ K in Fig. 3. The transition from the bulk PC liquid to the liquid strongly confined

to the polymer gel is not uniform. There are regions where the relaxation times show a rapid increase, from pure PC to about 13% PMMA and from 22% to about 32% PMMA content. However, the relaxation time is almost independent of the PMMA concentration in the region from 13% to 22% regarding w_{PMMA} . A very similar tendency has been observed by Svanberg *et al.* by dielectric spectroscopy on PC/PMMA gels.³⁰ It is concluded that the larger τ'_0 s reflect those of the polymer chain segments in a solvent-altered environment and the smaller τ'_0 s relate more to the solvent mobility in the presence of polymer chains.⁵¹ Compared with the dielectric measurement, the solvation technique is expected to respond more selectively to the dynamics of the PC molecules. The reason for this is the predominantly dipolar nature of the solvation of QX and the preferred solution in more polar solvents. In the present case, PC will generate the higher dipole density near QX. As a result, the range of the plateau phenomenon is less pronounced in the present case.

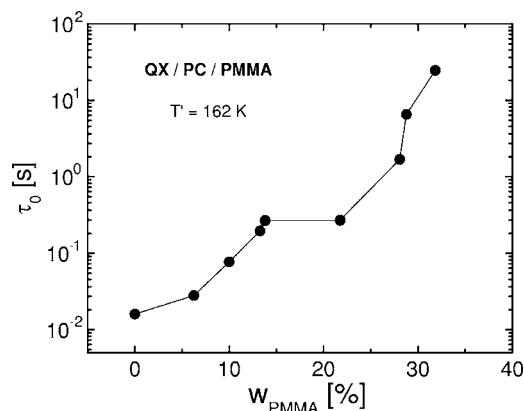


FIG. 3. Composition dependence of the solvent relaxation time τ_0 of QX in PC/PMMA, determined at a common temperature $T'=162$ K. Symbols represent the experimental results, the lines serve as guide only. In this range of PMMA weight fraction from 0 to 31.8%, the relaxation time changes a factor of 1540, i.e., approximately 3.2 decades.

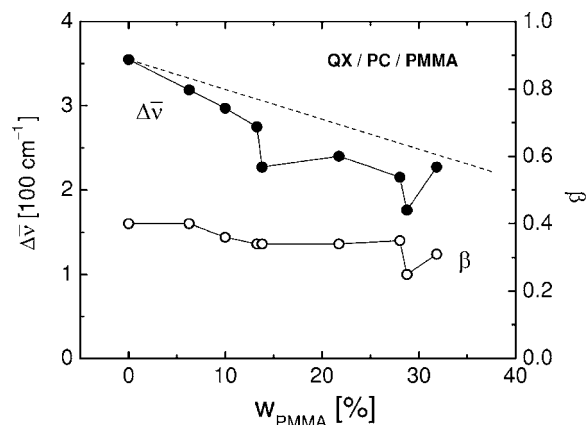


FIG. 4. Composition dependence of the total solvation redshift $\Delta\bar{\nu}$ (solid symbols) and stretching exponent β (open symbols) for the solvation dynamics of QX in PC/PMMA. Within the present experimental range, both values are considered temperature independent. The connecting lines serve as guides only, the dashed line shows $w_{\text{PC}} \times \Delta\bar{\nu}_{\text{bulk}}$, with $\Delta\bar{\nu}_{\text{bulk}}=355 \text{ cm}^{-1}$.

Apart from the average relaxation time, the redshift amplitude $\Delta\bar{\nu}$ and the stretching exponent β are quantities that change systematically with composition. With the addition of PMMA, the solvation amplitude is reduced from $\Delta\bar{\nu}_{\text{bulk}} = 355 \text{ cm}^{-1}$ to values around $\Delta\bar{\nu} \approx 200 \text{ cm}^{-1}$ at 32 wt. % PMMA. The dashed line in Fig. 4 shows $w_{\text{PC}} \times \Delta\bar{\nu}_{\text{bulk}}$, suggesting that the reduction of the polar (PC) component in the mixture could account for this effect. As in many examples, the dispersion of solvation times gauged by $\beta_{\text{bulk}} = 0.4$ is more pronounced than that of the dielectric relaxation.⁵² As the polymer is added, relaxation time gradients and concentration fluctuations are expected to add to the dispersion, which widens the distribution of relaxation times and reduces β to 0.3. In terms of dielectric relaxation data, pure PC displays an unusually high exponent $\beta \approx 0.73$ (relative to its fragility), so that concentration fluctuations become very apparent.³⁰ With the solvation dynamics counterpart, $\beta_{\text{bulk}} = 0.4$, as an upper limit for the composition dependence, the changes of β with w_{PMMA} are much smaller in a solvation study.

For assessing the effect of the cooperativity length scale ξ in this polymer solution, a translation from composition to an average PC-PMMA distance is required. However, the structure of polymers in solution is too complicated for a straightforward but realistic approach to the distribution of solvent molecule to polymer chain distances. In order to provide an estimate, we assume the picture that the macromolecules are parallel and equally spaced cylindrical rods in the liquid. Assuming a volume fraction P of PMMA in a liquid volume which is cubic with side length L , then the volume occupied by the polymer within the cube is

$$PL^3 = n\pi r^2 L. \quad (4)$$

Here, n is the number of polymer chains in the cube, $r \approx 0.25 \text{ nm}$ is the radius of the PMMA chain. In this approximation, the nearest center-to-center distance D between two polymer chains is simply

$$D = \frac{L}{\sqrt{n}} = \sqrt{\frac{\pi r^2}{P}}. \quad (5)$$

If the chromophore QX is uniformly dissolved in PC, the average distance x of one QX molecule to the nearest polymer chain is about half of that between two polymer chains after subtracting the radius r of the polymer chain. Table I includes these calculated distances x for the experimentally realized compositions. The value D for the 31.8% PMMA/PC sample is consistent with the polymer-polymer center of mass distance of 0.8 nm obtained from quasi-elastic neutron scattering experiments for a 30 wt. % PMMA/PC sample.⁵³ A more detailed scrutiny of polymer concentration effects has to go beyond a simple distance dependence: As the polymer content increases, the effective dimensionality of the confining topology will change from one- to more three-dimensional restrictions. In parallel, the more pronounced effects of binary and ternary contact points in a polymer solution gain importance. In a detailed structural study, Svanberg *et al.* have obtained the complex dependence of the “mesh” size in a polymer solution on its

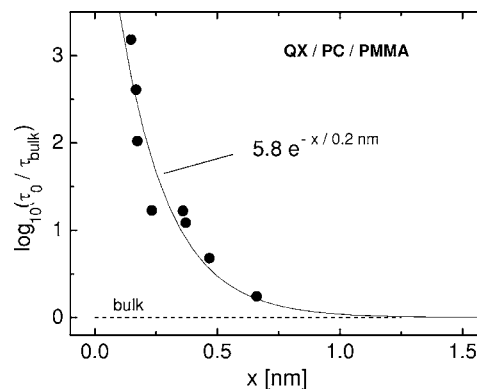


FIG. 5. Logarithmic ratio of the solvent relaxation time τ_0 ($T = 162 \text{ K}$) relative to the bulk value τ_{bulk} , plotted versus the estimated PC to nearest PMMA distance x . Symbols represent the experimental results, the solid line shows the relation $\log_{10}(\tau_0/\tau_{\text{bulk}}) = 5.8 \exp(-x/0.2 \text{ nm})$, the dashed line marks the bulk level $\tau_0 = \tau_{\text{bulk}}$.

concentration.⁵⁴ The resulting rapidity of the change of size with weight fraction is supportive of our above simplified estimate in the present composition range of interest.

The main implication of the above calculation is shown in Fig. 5, which shows that the relaxation time of PC increases sharply as the proximity to the polymer chain becomes more important. Empirically, the data can be described by the expression $\log_{10}(\tau_0/\tau_{\text{bulk}}) = 5.8 \exp(-x/0.2 \text{ nm})$, included in Fig. 5 as solid line. Two features of this graph are important: the total range of observed relaxation time change is 3.2 decades, and thus very similar to the total changes seen or estimated in other cases of confinement,⁵⁵ and the curve falls off much steeper than expected on the basis of typical values for the length scale of cooperativity, $\xi \approx 2 \pm 1 \text{ nm}$. In previous work on confined 3-methylpentane,²⁵ we have explored the dynamics of nanoconfined and interfacial supercooled liquids near their glass transition temperatures using porous glasses. By specifically measuring the dynamics of the interfacial layer at the pore wall,²³ it was found that the relaxation time is 3.3 orders of magnitude longer than that of the bulk liquid. Judged by the pore size effect, this frustration effect decreases gradually across the first few nanometers distance away from the interface. For supercooled propylene glycol in hard and soft confinement of porous glass microemulsion droplets, the observations are again consistent with a ≈ 3 decade change of the time scale at the interface and bulklike dynamics a distance ξ away from the surface.⁵⁵ The dynamics of PC in the highest PMMA concentration is again about 3 orders of magnitude slower compared with the bulk PC case. The 32 wt. % PMMA concentration might be similar to the situation of interfacial dynamics in pores, where one side of the environment is rigid (PMMA) while the remainder is mostly liquid (PC). Interestingly, a similar effect has been derived from a confined binary Lennard-Jones model of a liquid by Scheidler *et al.*,⁵⁶ which also displays a gradual change in relaxation time by three orders of magnitude as the surface is approached.

At distances further away from the polymer strands, the frustration effect of the PC/PMMA interface naturally de-

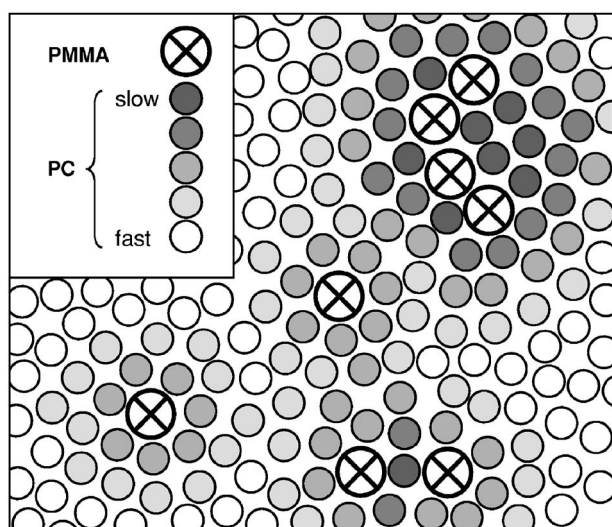


FIG. 6. Schematic view of how the solvent dynamics are modified by the presence of single, paired, and more clustered polymer strands. The polymer chains are assumed to intersect the drawing plane in a perpendicular manner. See legend for the identification of molecules and time scales. An important feature of this picture is that the slowest dynamics of the system are not found near a single chain but only in the more concentrated polymer environments.

creases. Previous studies concerned with the distance dependence from a surface were consistent with the cooperativity governing how the change in dynamics fades as the distance from the interface increases.^{25,55} The basis for this picture is that the distance ξ at which two molecules can relax independently should be also relevant for the separation between a molecule and a surface required for independent motion. However, the distance dependence in Fig. 5 appears to be significantly different than what has been observed for confinement to porous glasses or microemulsions. In order to explain the origin of the steepness characterized by the “ $1/e$ ” length of 0.2 nm, we note that the increase of the average distance is not the only consequence of varying the composition. At a lowered PMMA concentration, the amount of immobile material is not only more distant from PC (on average) but also more scattered and less interconnected. Therefore, it becomes evident that at a given distance from a molecule, a certain surface coverage is needed to generate the dramatic confinement effects observed in nanoscale pores. Because this surface coverage decreases with polymer

concentration, the abscissa in Fig. 5 is not a true spatial scale and the relaxation time reverts to the bulk value much more rapidly than on a real distance scale. Contrary to the picture advanced earlier (Fig. 7 of Ref. 30), we conclude that even the immediate proximity to a macromolecular chain is not sufficient for increasing the time scale by a factor of 1000 or more. Figure 6 provides an attempt to emphasize this view schematically, suggesting that the very slow dynamics will be found only near clustered polymer chains (top right situation). A better understanding and insight than currently available is needed for a more quantitative treatment of this interesting problem.

V. SUMMARY AND CONCLUSIONS

We have performed a triplet state solvation dynamics study of viscous propylene carbonate subject to the confinement effects imposed by the presence of up to 32 wt. % of a polymer, poly(methyl methacrylate). Consistent with a previous dielectric study of PC/PMMA, we observe a change in the solvent’s relaxation time by 3.2 orders of magnitude across the 0 to 0.32 PMMA weight fraction range. The extent of relaxation time change (factor of 1000–2000) appears to be a common feature for the frustration effect in the immediate vicinity of a rigid surface. A striking result is the rapidity with which the dynamics revert to bulk behavior as the PMMA concentration is reduced. This finding is not compatible with a pure PC-PMMA distance effect, where the length scale ξ of cooperativity governs the size or concentration dependence. Instead, close proximity to a polymer chain is assumed to generate only a fraction of the total change in dynamics, whereas a higher amount or surface coverage of the more rigid macromolecule is required around a solvent molecule in order to reduce its mobility by >3 orders of magnitude. Therefore, reducing the polymer concentration increases the average PC-PMMA distance and changes the confining topology from connected and extended rigid surfaces towards more molecule-sized immobile obstacles.

ACKNOWLEDGMENTS

The authors thank G. B. McKenna for information and support regarding polymers and polymer solutions, M. Thorpe for discussions on chain topologies, and C. Svanberg for the access to results prior to their publication. This material is based upon work supported by the National Science Foundation under Grant No. DMR 0304640 (NIRT).

¹C. A. Angell, K. L. Ngai, G. B. McKenna, P. F. McMillan, and S. W. Martin, *J. Appl. Phys.* **88**, 3113 (2000).

²G. Adam and J. H. Gibbs, *J. Chem. Phys.* **43**, 139 (1965).

³K. Schmidt-Rohr and H. W. Spiess, *Phys. Rev. Lett.* **66**, 3020 (1991).

⁴M. D. Ediger, *Annu. Rev. Phys. Chem.* **51**, 99 (2000).

⁵R. Richert, *J. Phys.: Condens. Matter* **14**, R703 (2002).

⁶E. W. Fischer, E. Donth, and W. Steffen, *Phys. Rev. Lett.* **68**, 2344 (1992).

⁷U. Tracht, M. Wilhelm, A. Heuer, H. Feng, K. Schmidt-Rohr, and H. W. Spiess, *Phys. Rev. Lett.* **81**, 2727 (1998).

⁸*Molecular Dynamics in Restricted Geometries*, edited by J. M. Drake and J. Klafter (Wiley, New York, 1989).

⁹A. Patkowski, T. Ruths, and E. W. Fischer, *Phys. Rev. E* **67**, 021501 (2003).

¹⁰J. Van Alsten and S. Granick, *Phys. Rev. Lett.* **61**, 2570 (1988); S. Granick, *Science* **253**, 1374 (1991).

¹¹R. G. Horn and J. N. Israelachvili, *J. Chem. Phys.* **75**, 1400

- (1981); J. N. Israelachvili and P. M. McGuiggan, *Science* **241**, 795 (1988).
- ¹²D. D. Awschalom and J. Warnock, *Phys. Rev. B* **35**, 6779 (1987).
- ¹³G. B. McKenna, *J. Phys. IV* **10**, Pr7-53 (2000).
- ¹⁴M. Alcoutlabi and G. B. McKenna, *J. Phys.: Condens. Matter* **17**, R461 (2005).
- ¹⁵C. L. Jackson and G. B. McKenna, *J. Non-Cryst. Solids* **131-133**, 221 (1991).
- ¹⁶M. D. Ediger, C. A. Angell, and S. R. Nagel, *J. Phys. Chem.* **100**, 13200 (1996).
- ¹⁷R. Richert, *Phys. Rev. B* **54**, 15762 (1996).
- ¹⁸D. M. Willard, R. E. Riter, and N. E. Levinger, *J. Am. Chem. Soc.* **120**, 4151 (1998).
- ¹⁹C. Streck, Yu. B. Mel'nichenko, and R. Richert, *Phys. Rev. B* **53**, 5341 (1996).
- ²⁰H. Wendt and R. Richert, *J. Phys.: Condens. Matter* **11**, A199 (1999).
- ²¹R. Richert, F. Stickel, R. S. Fee, and M. Maroncelli, *Chem. Phys. Lett.* **229**, 302 (1994).
- ²²R. Richert, *J. Chem. Phys.* **113**, 8404 (2000).
- ²³R. Richert and M. Yang, *J. Phys. Chem. B* **107**, 895 (2003).
- ²⁴L.-M. Wang, F. He, and R. Richert, *Phys. Rev. Lett.* **92**, 095701 (2004).
- ²⁵F. He, L.-M. Wang, and R. Richert, *Phys. Rev. B* **71**, 144205 (2005).
- ²⁶A. Scodinu, R. A. Farrer, and J. T. Fourkas, *J. Phys. Chem. B* **106**, 12863 (2002).
- ²⁷B. J. Loughnane, A. Scodinu, and J. T. Fourkas, *J. Phys. Chem. B* **103**, 6061 (1999).
- ²⁸R. A. Farrer, B. J. Loughnane, and J. T. Fourkas, *J. Phys. Chem. A* **101**, 4005 (1997).
- ²⁹S. Takahara, O. Yamamuro, and T. Matsuo, *J. Phys. Chem.* **99**, 9589 (1995).
- ³⁰C. Svanberg, R. Bergman, P. Jacobsson, and L. Börjesson, *Phys. Rev. B* **66**, 054304 (2002).
- ³¹M. Maroncelli, *J. Mol. Liq.* **57**, 1 (1993).
- ³²G. R. Fleming and M. Cho, *Annu. Rev. Phys. Chem.* **47**, 109 (1996).
- ³³F. Stickel, E. W. Fischer, and R. Richert, *J. Chem. Phys.* **104**, 2043 (1996).
- ³⁴T. G. Fox and L. Loshaek, *J. Polym. Sci.* **15**, 371 (1955).
- ³⁵G. Carini, V. Crupi, G. D'Angelo, D. Majolino, P. Migliardo, and Yu. B. Mel'nichenko, *J. Chem. Phys.* **107**, 2292 (1997).
- ³⁶M. D'Angelo, D. Fioretto, G. Onori, and A. Santucci, *Phys. Rev. E* **58**, 7657 (1998).
- ³⁷Yu. B. Mel'nichenko, J. Schüller, R. Richert, B. Ewen, and C.-K. Loong, *J. Chem. Phys.* **103**, 2016 (1995).
- ³⁸Y. Ryabov, A. Gutina, V. Arkhipov, and Y. Feldman, *J. Phys. Chem. B* **105**, 1845 (2001).
- ³⁹J. Schüller, R. Richert, and E. W. Fischer, *Phys. Rev. B* **52**, 15232 (1995).
- ⁴⁰R. M. Dickson, D. J. Norris, Y.-L. Tzeng, and W. E. Moerner, *Science* **274**, 966 (1996).
- ⁴¹J. Y. Park and G. B. McKenna, *Phys. Rev. B* **61**, 6667 (2000).
- ⁴²A. Huwe, F. Kremer, P. Behrens, and W. Schwieger, *Phys. Rev. Lett.* **82**, 2338 (1999).
- ⁴³R. Bergman, J. Swenson, L. Börjesson, and P. Jacobsson, *J. Chem. Phys.* **113**, 357 (2000).
- ⁴⁴G. Barut, P. Pissis, R. Pelster, and G. Nimtz, *Phys. Rev. Lett.* **80**, 3543 (1998).
- ⁴⁵A. Huwe, M. Arndt, F. Kremer, C. Haggemüller, and P. Behrens, *J. Chem. Phys.* **107**, 9699 (1997).
- ⁴⁶H. Wendt and R. Richert, *J. Phys. IV* **10**, Pr7-67 (2000).
- ⁴⁷G. Barut, P. Pissis, R. Pelster, and G. Nimtz, *Phys. Rev. Lett.* **80**, 3543 (1998).
- ⁴⁸M. Yang and R. Richert, *Chem. Phys.* **284**, 103 (2002).
- ⁴⁹L.-M. Wang and R. Richert, *J. Chem. Phys.* **120**, 11082 (2004).
- ⁵⁰G. Floudas, W. Steffen, E. W. Fischer, and W. Brown, *J. Chem. Phys.* **99**, 695 (1993).
- ⁵¹D. J. Plazek and K. L. Ngai, in: *Physical Properties of Polymers Handbook*, edited by J. E. Mark (AIP, Woodbury, NY, 1996), Chap. 12.
- ⁵²N. Ito, K. Duvvuri, D. V. Matyushov, and R. Richert, *J. Chem. Phys.* (to be published).
- ⁵³C. Svanberg, W. Pyckhout-Hintzen, and L. Börjesson, *Electrochim. Acta* **51**, 4153 (2006).
- ⁵⁴T. Uematsu, C. Svanberg, M. Nyden, and P. Jacobsson, *Phys. Rev. E* **68**, 051803 (2003).
- ⁵⁵F. He, L.-M. Wang, and R. Richert, *J. Phys. IV* (to be published).
- ⁵⁶P. Scheidler, W. Kob, and K. Binder, *Europhys. Lett.* **52**, 277 (2000).